# Fault Diagnosis for Buckling Friction Components in Wet Multi-Disc Clutches Using IHHT

Yuqing Feng, Changsong Zheng, Liang Yu<sup>✉</sup>, Chengsi Wei, Xiangjun Ouyang

**Abstract:** The wet multi-disc clutches are extensively used in various transmission systems, with one of the most prevalent failure modes being the buckling deformation of friction components. An improved Hilbert-Huang transform method (IHHT) is proposed to address the limitations of traditional time-domain vibration analyses, such as low accuracy and mode mixing. This paper first classifies the buckling degree of the friction components. Next, wavelet packet transform (WPT) is applied to the vibration signals of different buckling plates to partition them into distinct frequency bands. Then, the instantaneous features are extracted by empirical mode decomposition (EMD) and Hilbert transform (HT) to discarding extraneous intrinsic mode function (IMF) components. Comparative analyses of Hilbert spectral entropy and time-domain features confirm the enhanced precision of IHHT under specific classifiers, which is better than traditional methods.

**Keywords:** multi-disc clutch; buckling; fault diagnosis; Hilbert-Huang transform; entropy

## 1 Introduction

As an important part of the vehicle transmission, the wet multi-disc clutch is responsible for the crucial task of power transmission, which means it transmits high-power torque or cuts off the power in emergency. Due to the compact structure, easy handling, and high power transmission capacity, it is widely used in the comprehensive transmission of various vehicles [1]. As shown in Fig. 1, the multi-disc clutch is mainly composed of the cylinder liner, piston, friction disc, separate plate, and back plate, with the friction discs and separate plates arranged alternately. During the engagement, the friction components gradually approach and slide against

each other under oil pressure to facilitate power transmission. The duration of the process is usually within 1 s. Therefore, the short-term sliding process generates a large amount of heat, which cannot be dissipated in a timely manner. The friction component is forced to absorb this part of energy and the huge engagement pressure simultaneously. Under the dual action of thermal and mechanical stress, buckling deformation or local hot spots can easily occur, resulting in performance degradation, even failure [2]. Such phenomenon is considered one of the main forms of friction component failure modes, and its impact on the usage function and vehicle safety cannot be ignored.

Researchers have carried out extensive theoretical and experimental investigations. In the 1980s, Zagrodzki et al. used numerical methods to study the temperature field of the clutch, and found a dishing failure mode, namely buckling [3]. Considering the uneven contact caused by the buckling deformation, the hot spot phenomenon was then studied in detail [4]. Xiong et al. calculated the critical in-plane bending
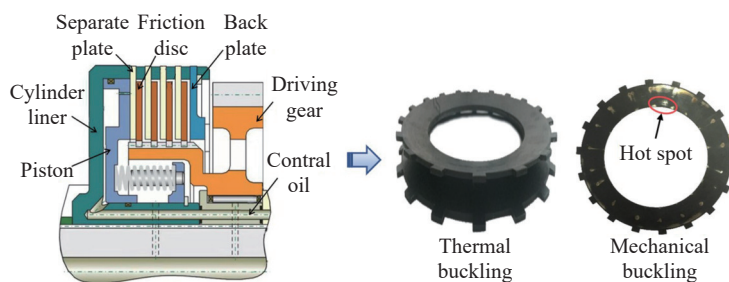
Fig. 1    Illustration of wet multi-disc clutch

moment by using the curved beam model and predicted the buckling behavior by combining the thermal stress [5]. A mechanical buckling model of separate plate was established in [6], and the results showed that high resistance torque was the main reason for the high-order circumferential buckling in the separate plate. By using the Mindlin plate theory and the axisymmetric flatness conditions, Bagheri et al. found that the critical buckling torque and its shape depended on the boundary conditions, radius ratio, and thickness ratio [7]. The buckling deformation will not only affect the temperature distribution and wear unevenness but also reduce the working performance and the lifespan. Therefore, it is both urgent and challenging to conduct research aimed at formulating an effective buckling diagnosis method.

In recent years, data-driven fault diagnosis and machine learning methods have developed rapidly and have been proven to be beneficial for device prediction and health management [8–10]. Daubechies et al. provided a mathematical definition for the components of empirical mode decomposition (EMD) based on wavelet analysis and repositioning methods, avoiding the problem of component overlap caused by EMD in vibration signal decomposition [11]. Chen et al. used short-time Fourier transform (STFT) to analyze frequency spectrum differences in the shifting clutch before and after shifting, proving that this method can achieve qualitative analysis of early faults. In terms of machine learning, Senatore et al. obtained a comprehensive view of the influence of clutch master slip parameters through

artificial neural networks to improve friction coefficient prediction during transient operation [12]. A deep normalized convolutional neural network (DNCNN) was proposed by [13] for imbalanced fault classification of machines. Despite the advances in diagnosis methods for rotating machinery such as bearings and gearboxes, there has been little research on wet clutch. The working environment and operating state of multi-disc clutches are relatively complex, and the kinematic property at high speeds remains unclear [14].

Based on this, a fault diagnosis method based on the improved Hilbert-Huang transform is proposed in this paper. The time-frequency entropy and multiple time-domain features are used as the main parameters of multi-disc wet clutch buckling diagnosis to realize classification of fault degree. The paper is arranged as follows. Section 2 introduces the causes and effects of the friction component buckling, and then the buckled discs are divided into three classes based on the three dimensional (3D) measurement, namely health, medium buckling and severe buckling. Section 3 presents the experimental scheme design, then applies the improved method to decompose and reconstruct the vibration data, addressing issues related to mode mixing and pseudo-intrinsic mode functions (IMFs), and then calculates the time-frequency entropy of the Hilbert spectrum. Section 4 applies five classifiers, using time-frequency entropy and time-domain features as inputs for fault classification, and the effectiveness is verified afterwards. Section 5 summarizes the researches done in this paper finally.

## 2 Gradation of Buckling Height

### 2.1 The Impact of Buckling

Elastic or plastic buckling deformation of friction components has a series of effects on the dynamic and working characteristics of multi-disc clutch, as shown in Fig. 2. First, the buckled friction components lead to the uneven distribution of contact area and pressure, resulting in increased noise and vibration. Second, the axial buckling occupies the normal gap after fully separation, causing contact sliding and collision among adjacent friction components under non-operational conditions. Third, buckled discs alter the torsional stiffness and stiffness distribution of the material, resulting in diminished dynamic response [15]. Therefore, timely monitoring and maintenance of friction components are essential to ensure operation and extend its life cycle.
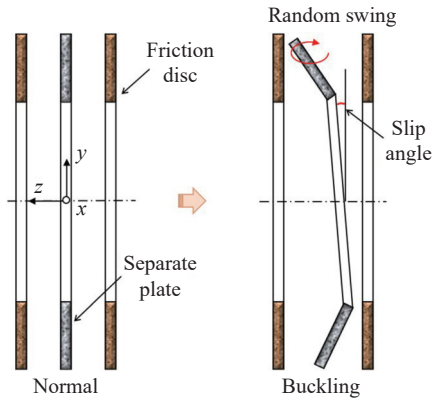


Fig. 2    Diagram of buckled separate plate

### 2.2 Buckling Degree Definition

The Creaform Handy 3D scanner is utilized to measure the buckling height of the friction components, as detailed in [16]. This paper categorizes the buckled discs into three classes: health (H), medium buckling (M), and severe buckling (S) [17]. The average buckling height and angle of friction components are shown in Tab. 1. It can be seen that the buckling height and angle of Class M and Class S are significantly larger than those of Class H, which is conducive to the subsequent work. In addition, disassembly test of the clutch pack reveals that buckling deformation is more likely to occur in the separate plate. Therefore, the following research will focus on the buckled separate plate. It should be noted that the friction components mentioned henceforth refer to the separate plate specifically.

Tab. 1  Buckling state

| Buckling degree | Buckling height (mm) | Buckling angle (°) |
|---|---|---|
| Health (H) | 0.36 | 0.53 |
| Medium (M) | 2.16 | 3.17 |
| Severe (S) | 4.52 | 6.61 |

## 3 Experimental Analysis and Data Processing

### 3.1 Test Scheme Design

The layout of the test rig is shown in Fig. 3. It is mainly composed of a motor, a braking system, a clutch pack, and data acquisition equipment. The motor provides the power input to bring the clutch up to a predetermined speed. The clutch pack, comprising friction components in proportions, includes a buckled separate plate and healthy friction discs made of 65Mn and copper-based steel, respectively. The brake is fixedly connected to the output shaft of the clutch pack. The data acquisition equipment, comprising an axial acceleration sensor, a speed sensor, and a personal computer (PC), collects rotation speed and vibration signals. According to [18], the buckled separate plate and the acceleration sensor are positioned on the side near the circlip.

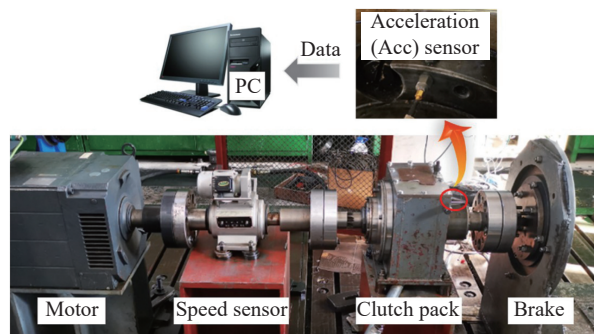For the experimental parameter settings, the



Fig. 3    The layout of test rig and signal system

initial temperature for automatic transmission fluid (ATF) is 30 ℃. The motor's rated power is 205 kW, with variable frequency and adjustable speed. The vibration data is collected at a sampling frequency of 65 536 Hz, and then processed through the B&K PULSE software on the PC end. According to the commonly used speed of wet clutches, a total of six different speed settings are established, ranging from 600 revolutions per minute (r/min) to 1600 r/min, with 200 r/min intervals. Comparative tests are conducted sequentially for Class H, Class M, and Class S, comprising a total of 18 groups. Each condition is maintained for 5 s and repeated three times. The specific test parameters are detailed in Tab. 2.

**Tab. 2  Experimental parameter configuration**

| Parameter | Value |
|---|---|
| Inner radius (mm) | 86 |
| Outer radius (mm) | 125 |
| Thickness (mm) | 2 |
| ATF temperature (℃) | 30 |
| Rotating speed (r/min) | 600, 800, 1 000, 1 200, 1 400, 1 600 |
| Engagement time (s) | 5 (repeat 3 times) |
| Sampling frequency (Hz) | 65 536 |
| Motor power (kW) | 205 |
| Buckling class | H, M, S |

### 3.2  Improved Method Based on Hilbert-Huang Transform

The original vibration signals of Class H and Class S at 800 r/min are shown in Fig. 4. It is evident that the original data contain a significant amount of white noise and interference signals, making it impractical to directly extract fault features associated with different levels of buckling. The impact generated by the buckled friction components in their separated state resembles a pulse signal, leading to a sudden change in the signal's amplitude. This change disrupts its continuity at this point — a phenomenon known as the first type of discontinuity.

The random local collision energy generated by the buckling of friction components is often non-stationary and small, making it easily submerged within the energy spectrum of the entire signal. Traditional methods in the time or frequency domain (such as STFT) only provide a one-dimensional representation of signal variations over time or frequency, thus failing to capture precise instantaneous characteristics of signals, especially when analyzing complex signals containing variations across multiple frequency components [19]. Therefore, traditional methods lack the capability for quantitative fault analysis. Time-frequency analysis methods, such as wavelet transform and Hilbert-Huang transform (HHT), can offer local time-frequency characteristics and instantaneous events of signals simultaneously. Certainly, HHT also has its drawbacks, such as the generation of spurious IMF components and mode mixing issues after EMD processing.
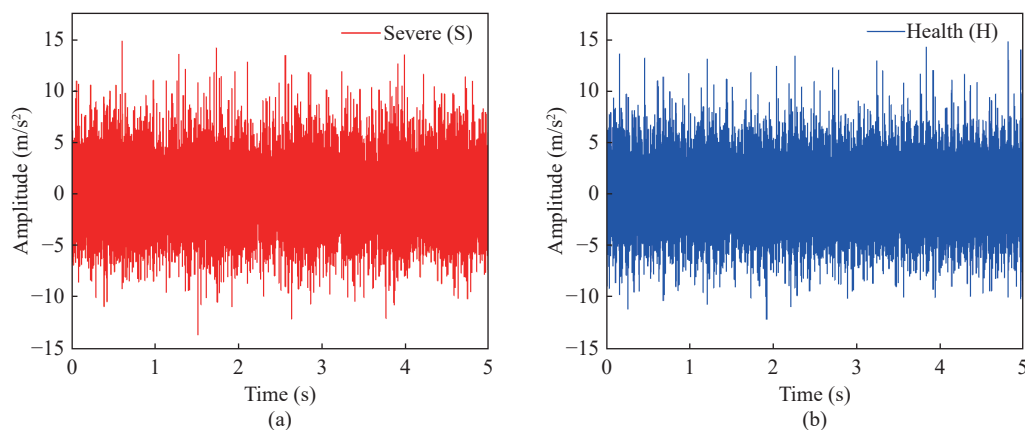


Fig. 4    Original signals of 800 r/min: (a) Class H; (b) Class S

Therefore, this paper combines wavelet packet transform (WPT) and HHT to capture the impulsive signals and local discontinuities caused by buckling deformations and more effectively analyze modal mixing and nonlinear features in complex signals. The WPT preliminarily partitions the frequency of the clutch vibration signals and reduces the initial bandwidth, enhancing the precision and robustness of signal decomposition to mitigate the shortcomings of HHT. Based on the frequency range and transient features of the target signal, this paper selects the three-layer Symlet 4 (sym4) wavelet base, which effectively captures the mutations or spikes that occur during the faults. The signal is decomposed into multiple levels across different frequency bands, showing a strong time-frequency localization capability. The architecture of the proposed method is shown in Fig. 5. Tak-

ing the three-layer WPT as an example, the signal decomposition is defined as follows

$$
\begin{aligned}
\mathrm{RS} = &\mathrm{RH}_{0,0} + \mathrm{RL}_{0,0} + \mathrm{RH}_{0,1} + \mathrm{RL}_{0,1} + \mathrm{RH}_{1,0} + \\
&\mathrm{RL}_{1,0} + \mathrm{RH}_{1,1} + \mathrm{RL}_{1,1}
\end{aligned} \tag{1}
$$

where RS is the original signal, $\mathrm{RH}_{i,j}$ and $\mathrm{RL}_{i,j}$ ($i$, $j = 0$, $1$) are the high-frequency and low-frequency fragments respectively.

Before signal processing, all original signals are divided into 40 smaller segments, each lasting for 0.125 s (with a rotation angle greater than 360° at 600 r/min), and signals below 1 kHz are filtered out [17]. Then, the segmented signals are subjected to HHT, including EMD and Hilbert transform (HT) processes. Initially, EMD is performed to obtain several IMFs, ranging from high to low frequencies. The signal is then reconstructed by discarding non-contributory IMF components and processed through HT to yield the Hilbert spectrum. This method effec-
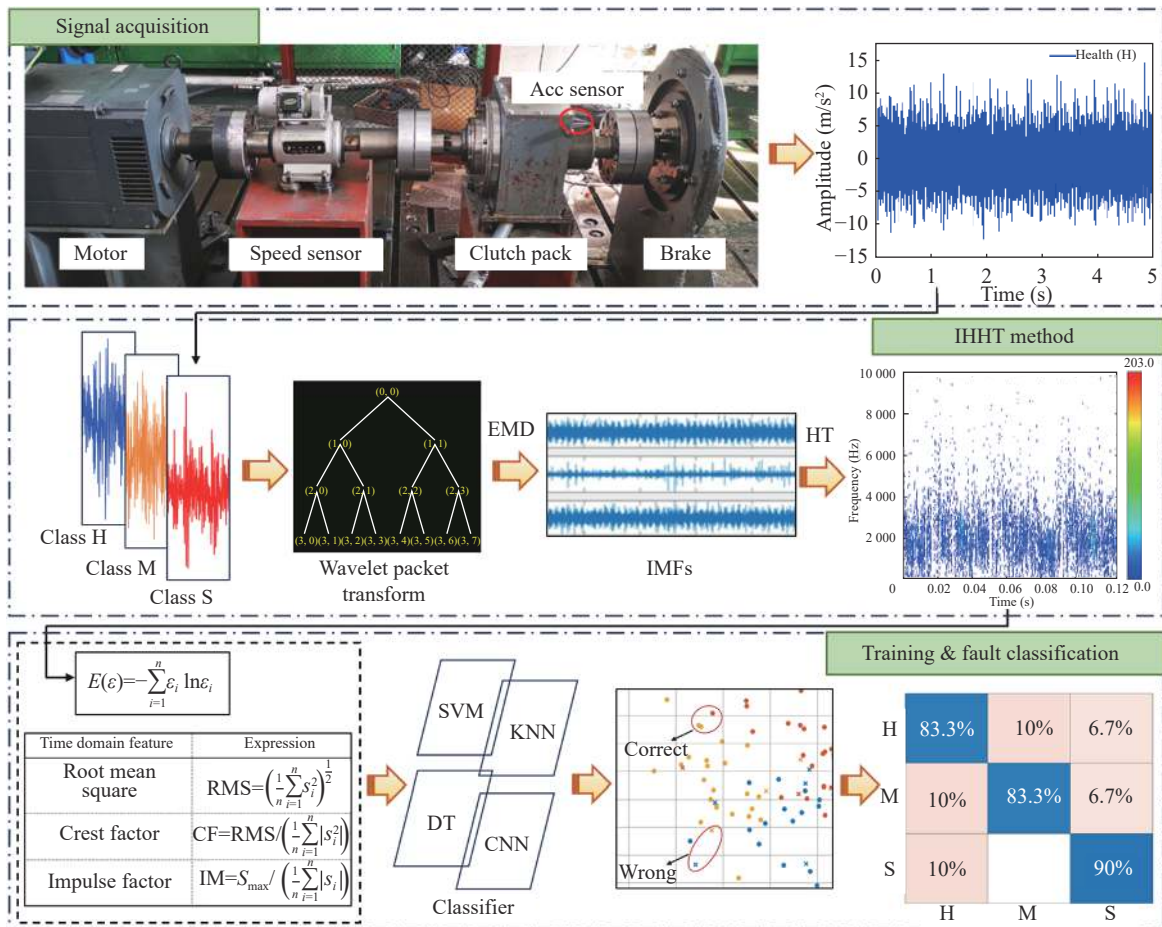


Fig. 5　Architecture of the proposed fault diagnosis method

tively addresses the issue of negative frequencies, ensuring the extraction of physically meaningful positive instantaneous frequencies for accurate time-frequency analysis. The improved Hilbert-Huang transform method (IHHT) flow chart is shown in Fig. 6. The Hilbert spectrum can be expressed as

$$H\left(\alpha,t\right)=\mathrm{Re}\sum_{i=1}^{n}b_{i}\left(t\right)\mathrm{e}^{\mathrm{j}\int\alpha_{i}(t)\mathrm{d}t} \qquad (2)$$

where Re is the operator of the real part, $b_i(t)$ represents the amplitude, and $\alpha_i(t)$ is the instantaneous frequency.
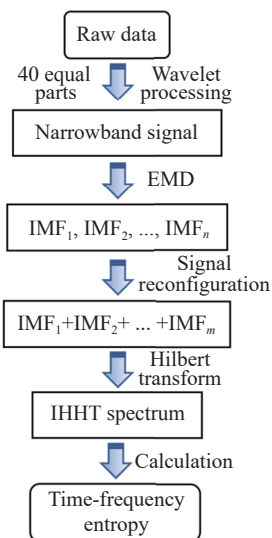


Fig. 6    Flowchart of the improved Hilbert-Huang transform

The Hilbert spectrum for Class S at 800 r/min is shown in Fig. 7, where the *X*-axis represents the time and the *Y*-axis represents the frequency.
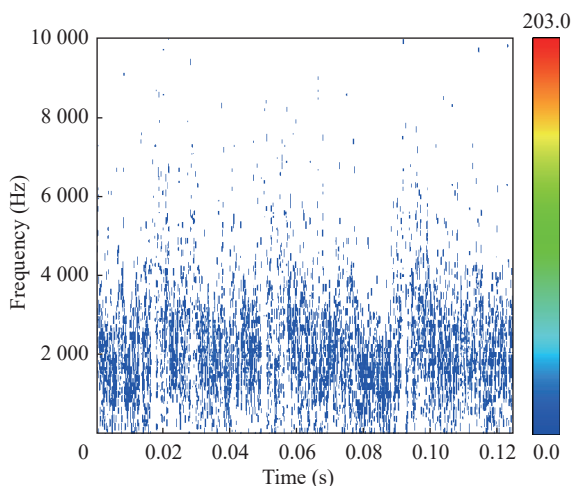


Fig. 7    Hilbert spectrum of Class S at 800 r/min

The varying colors correspond to the power intensity of vibration at specific times and frequencies. The Hilbert spectrum visually reveals the variances in frequency components and energy density at different times, with high local energy values emerging at brief intervals. However, it falls short in quantitatively capturing the overall information.

### 3.3  Entropy Calculation

Given the slight differences in signal energy across various speeds and buckling classes, this paper introduces time-frequency entropy as an indicator to quantify the information and uncertainty contained within the signals. The time-frequency entropy of signal after IHHT can be expressed as

$$E\left(\varepsilon\right)=-\sum_{i=1}^{n}\varepsilon_{i}\ln\varepsilon_{i} \qquad (3)$$

where $E(\varepsilon)$ represents time-frequency entropy; $\sum_{i=1}^{n}\varepsilon_{i}=1\left(n=256\right)$, which satisfies the original normalization criterion.

Based on the test conditions, the time-frequency entropy of 480 sets of vibration data across the three buckling classes, ranging from 800 r/min to 1400 r/min, is calculated. The entropy value distribution is shown in Fig. 8. As the speed increases, the entropy values of different classes display a generally rising trend. The average value for Class H exceeds those of the other two classes, especially at 1200 r/min. Class
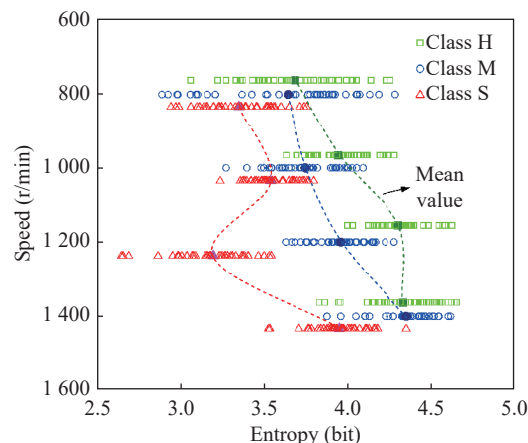


Fig. 8    Entropy values of different buckling classes

S shows a significant decrease at 1 200 r/min, indicating that the severely buckled separate plate has reached a certain "balanced" state at this speed. Overall, the entropy values of the three classes display clear distinction, which are beneficial for follow-up analyses.

# 4    Fault Diagnosis of Buckling Degree

## 4.1    Data Preparation

The data segmentation described in Section 3 aims to reduce internal duplicate information while increasing the number of samples. After segmentation, the 0.125 s data includes 8 192 sampling points, which is sufficient to contain the collision characteristics rotating for more than one cycle. Based on the time-frequency entropy, some commonly used time-domain features are also selected as auxiliary inputs for the model [16], including six types: root mean square (RMS), crest factor (CF), kurtosis (Kr), skewness (Sk), impulse factor (IM), and energy (Eg), as shown in Tab. 3. The crest factor, which is the ratio of the signal's peak to its effective value, describes peak characteristics. A larger crest factor indicates greater signal fluctuation. The impulse factor is the ratio of the peak value to the absolute average value. A larger value indicates a stronger impact.

**Tab. 3  Time-domain features used in fault classification**

| Time domain feature | Expression |
| --- | --- |
| Root mean square | $\mathrm{RMS} = \left( \dfrac{1}{n} \sum\limits_{i=1}^{n} s_i^2 \right)^{\frac{1}{2}}$ |
| Crest factor | $\mathrm{CF} = \mathrm{RMS} / \left( \dfrac{1}{n} \sum\limits_{i=1}^{n} |s_i| \right)$ |
| Impulse factor | $\mathrm{IM} = S_{\max} / \left( \dfrac{1}{n} \sum\limits_{i=1}^{n} |s_i| \right)$ |
| Kurtosis | $\mathrm{Kr} = \dfrac{1}{n} \sum\limits_{i=1}^{n} \dfrac{(s_i - \bar{s})^4}{\rho^4}$ |
| Skewness | $\mathrm{Sk} = \dfrac{1}{n} \sum\limits_{i=1}^{n} \dfrac{(s_i - \bar{s})^3}{\rho^3}$ |
| Energy | $\mathrm{Eg} = \sum\limits_{i=1}^{n} s_i^2$ |

Mechanical failure diagnosis methods based on machine learning have been gradually adopted by researchers, promoting the improvement of fault diagnosis level. Consequently, this paper selects three traditional machine learning methods (support vector machine (SVM), k-nearest neighbors (KNN), and decision tree (DT)), as well as the recently popular convolutional neural network (CNN) method for clutch buckling degree fault recognition and diagnosis. As known in Section 3.3, a total of 480 samples are obtained from the experiments ranging from 800 r/min to 1 400 r/min (each test including 120 samples). To verify the accuracy and robustness of different models under varying datasets and data volumes, two data utilization methods are designed. Firstly, 120 sets of data under different rotational speed conditions are utilized as a small dataset to analyze the performance of the model, with a training to validation set ratio of 3:1. Similarly, all the data (480 sets of samples) are employed as a large dataset to assess the model's classification performance, with the same proportion division as mentioned above. To ensure the credibility of the results, all training processes are subjected to 4-fold cross-validation to train the model, and the mean value of the results is taken to represent the final performance of the model.

## 4.2    Results Discussion

After the cross-validation process, the scatter diagram and confusion matrix obtained by SVM classifier at 1 400 r/min are shown in Fig. 9 and Fig. 10, respectively. In Fig. 9, the blue, yellow, and orange colors represent Class H, Class M,
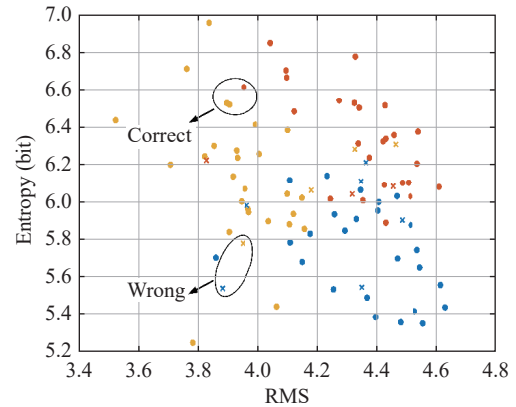


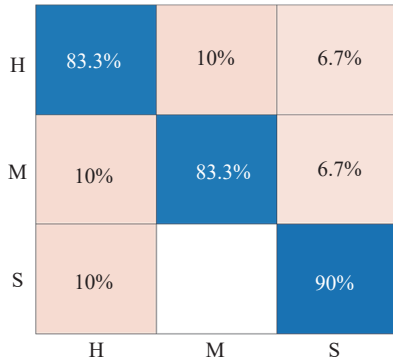Fig. 9    Scatter chart under SVM classifier

Fig. 10    Confusion matrix under SVM classifier

and Class S in turn. Among them, the circle symbolizes the correctly classified data, while the cross symbolizes data that has been misclassified to other degrees. Due to the diversity and randomness of vibration data, some deviation from normal feature data points is inevitable. As shown in Fig. 10, all three classes achieve a correct rate of over 83%, with Class S reaching as high as 90%. In addition, 10% of Class M is classified as healthy, and 6.7% as severe buckling. Similarly, 10% of Class S is misclassified as healthy state, which could be attributed to its motion characteristics resembling those of Class H at this velocity, aligning with the phenomena observed in the preceding chart.

Tab. 4 presents the predictive performance of different models on the small dataset. It should be noted that as a neural network, CNN requires some parameter settings before application. Based on experience and actual operation, the CNN classifier is configured with a two-layer structure, including two convolutional layers and two pooling layers, with a learning rate of 0.006, and 150 iterations. The rectified linear unit (ReLU) activation function is implemented to enhance the model's nonlinearity. Moreover, a

dropout mechanism is introduced to prevent overfitting during training, set at 0.3. It is evident that all four classifiers have achieved high accuracy. The CNN model shows the highest overall accuracy rate, mostly exceeding 90%. And it exhibits good robustness with an accuracy difference of only 8.8%, while other classifiers have a difference of 20% or more. Additionally, the accuracy of the four classifiers is the highest at 1200 r/min, followed by 800 r/min, suggesting that the vibrational characteristics of the buckled plates are more pronounced at these speeds. Overall, the performance of the classifier meets expectations, with CNN model performing the best at an average of 93.03%, followed by SVM at 87.55%.

To assess classifier performance on a larger dataset, all 480 set of samples are utilized. Due to the increased data volume, a fine-tuning of CNN parameters is necessary: the learning rate is adjusted to 0.008 and dropout to 0.4, with other parameters remaining unchanged. Fig. 11 and Tab. 5 present the predictive results of each classifier. It can be observed that the accuracy of the classifiers has improved, indicating that the increased data volume allows the model to fully learn the signal characteristics of different buckling degrees. The CNN continues to perform bet-



Fig. 11    Confusion matrix under CNN classifier

**Tab. 4  Accuracy of different classifiers**

| Classifier | Accuracy of different speeds (%) | | | |
| --- | --- | --- | --- | --- |
| | 800 r/min | 1 000 r/min | 1 200 r/min | 1 400 r/min |
| SVM | 90.2 | 74.4 | 100 | 85.6 |
| KNN | 95.1 | 75.6 | 95.6 | 73.3 |
| DT | 82 | 78.2 | 93.3 | 70 |
| CNN | 93.5 | 88.5 | 98.3 | 91.8 |

**Tab. 5  Accuracy of original and improved methods**

| Method | Classifier | | | |
| --- | --- | --- | --- | --- |
| | SVM | KNN | DT | CNN |
| HHT [17] | 92.5% | 89.4% | — | — |
| IHHT | 93.1% | 93.5% | 89.6% | 96.4% |

ter, achieving an accuracy rate of 96.4%, an improvement of 3.37% over the small dataset, followed by KNN with an accuracy of 93.5%. Overall, the CNN classifier shows the best performance in terms of accuracy and robustness. To demonstrate the superiority of the proposed IHHT method, the results are compared with the original HHT method in [16], as shown in Tab. 5. The IHHT method apparently improves classification accuracy, especially under the KNN, by nearly 4%. In summary, the IHHT method has proven its ability to accurately extract signal characteristics and facilitate buckling fault diagnosis under various conditions, enhancing both accuracy and robustness. In addition, striving for outstanding diagnostic precision under more comprehensive working conditions remains an urgent direction for future research.

# 5　Concluding Remarks

This article proposes an effective feature extraction method based on the improved Hilbert-Huang transform to address the challenges of identifying and diagnosing the vibration characteristics of the buckling faults in wet multi-disc clutch. The method adopts a combination of wavelet packet transform and Hilbert-Huang transform. To address the issues of mode mixing and pseudo-IMFs in the Hilbert-Huang transform, this study has implemented improvements through the use of wavelet packet decomposition. This enhancement aims to increase the accuracy of time-frequency analysis.

Building upon the previous research, separate plates with different buckling degrees are divided into three classes: health, medium buckling and severe buckling. Following this categorization, bench tests are systematically carried out with the specific aim of investigating the differential vibration characteristics elicited by different degrees of buckling. Then, the collected vibration data are applied to 3-layer wavelet packet decomposition and reconstruction. The

obtained series of narrow-band signals are performed Hilbert-Huang transform then to obtain the corresponding Hilbert spectrum. Finally, by combining the time-frequency entropy with the commonly used time-domain indicators as input parameters, four classifiers, including SVM, KNN, DT and CNN, are applied to validate the efficiency of the improved method compared to the original Hilbert-Huang transform.

The results show that the proposed improved method significantly enhances the classification accuracy and robustness. The CNN classifier performs the best under different working conditions and data volumes, with an average accuracy of over 93%. As the data volume increases, the accuracy improves to 96.4%. And the DT performs the worst, failing to learn enough buckling features. This achievement provides valuable guidance for monitoring and diagnosing the buckling faults of clutch. However, there are also certain limitations, namely how to reduce the probability of misclassification and find more effective feature extraction methods for the special working environment of wet multi-disc clutch, which is also the key point of future work.

# References：

[1]　L. Yu, B. Ma, C. Zheng, M. Chen, Q. Wang, and B. Zhang, "Study on the groove area effects on the friction-wear properties of a Cu-based wet clutch, " *Tribology International*, vol. 163, pp. 107096, 2021.

[2]　D. Wang, M. Hu, and D. Qin, "Cooperative effects of control parameters on the dynamic responses of vehicle powertrain during start-up process, " *Proceedings of the Institution of Mechanical Engineers, Part D: Journal of Automobile Engineering*, vol. 236, no. 13, pp. 2932-2948, 2022.

[3]　P. Zagrodzki, "Numerical analysis of temperature fields and thermal stresses in the friction discs of a multidisc wet clutch, " *Wear*, vol. 101, no. 3, pp. 255-271, 1985.

[4]　P. Zagrodzki and S. A. Truncone, "Generation of hot spots in a wet multidisk clutch during short-term engagement, " *Wear*, vol. 254, no. 5-6, pp. 474-

491, 2003.

[5] C. Xiong, B. Ma, H. Li, F. Zhang, and D. Wu, "Experimental study and thermal analysis on the buckling of friction components in multi-disc clutch, " *Journal of Thermal Stresses*, vol. 38, no. 11, pp. 1323-1343, 2015.

[6] L. Yu, B. Ma, M. Chen, H. Li, and J. Liu, "Investigation on the thermodynamic characteristics of the deformed separate plate in a multi-disc clutch, " *Engineering Failure Analysis*, vol. 110, pp. 104385, 2020.

[7] H. Bagheri, Y. Kiani, and M. R. Eslami, "Buckling of moderately thick annular plates subjected to torque, " *Archive of Mechanical Engineering*, vol. 66, no. 2, pp. 209-227, 2019.

[8] Y. Zhu, C. Zhu, J. Tan, Y. Tan, and L. Rao, "Anomaly detection and condition monitoring of wind turbine gearbox based on LSTM-FS and transfer learning, " *Renewable Energy*, vol. 189, pp. 90-103, 2022.

[9] M. Li, M. M. Khonsari, D. M. C. McCarthy, and J. Lundin, "On the wear prediction of the paper-based friction materialin a wet clutch, " *Wear*, vol. 334-335, pp. 56-66, 2015.

[10] K. C. Ganesh, K. Dhanasekaran, P. Saravanan, and R. Panda, "Failure analysis of multi plate wet-clutch used in off-highway transmission, " *Engineering Failure Analysis*, vol. 127, pp. 105534, 2021.

[11] I. Daubechies, J. Lu, and H. Wu, "Synchrosqueezed wavelet transforms: An empirical mode decomposition-like tool, " *Applied and Computational Harmonic Analysis*, vol. 30, no. 2, pp. 243-261, 2011.

[12] A. Senatore, V. D'Agostino, R. Di Giuda, and V. Petrone, "Experimental investigation and neural network prediction of brakes and clutch material frictional behaviour considering the sliding acceleration influence, " *Tribology International*, vol. 44, no. 10, pp. 1199-1207, 2011.

[13] F. Jia, Y. Lei, N. Lu, and S. Xing, "Deep normalized convolutional neural network for imbalanced fault classification of machinery and its understanding via visualization, " *Mechanical Systems and Signal Processing*, vol. 110, pp. 349-367, 2018.

[14] H. Bao, W. Huang, and F. Lu, "Investigation of engagement characteristics of a multi-disc wet friction clutch, " *Tribology International*, vol. 159, pp. 106940, 2021.

[15] N. Fatima, P. Marklund, and R. Larsson, "Influence of clutch output shaft inertia and stiffness on the performance of the wet clutch, " *Tribology Transactions*, vol. 56, no. 2, pp. 310-319, 2013.

[16] J. Xue, B. Ma, M. Chen, Q. Zhang, and L. Zheng, "Experimental investigation and fault diagnosis for buckled wet clutch based on multi-speed Hilbert spectrum entropy, " *Entropy*, vol. 23, no. 12, pp. 1704, 2021.

[17] Y. Qi, "Study on vibration characteristics of friction pairs deformation in wet shifting clutches, " Ph. D. dissertation, Beijing Institute of Technology, 2016.

[18] L. Yu, B. Ma, I. Y. Kim, and H. Li, "Influences of the uneven contact pressure and the initial temperature on the hot judder behavior in a multi-disc clutch, " *Proceedings of the Institution of Mechanical Engineers, Part J: Journal of Engineering Tribology*, vol. 234, no. 4, pp. 500-514, 2020.

[19] M. Chen, H. Li, B. Ma, and J. Zhao, "Initial malfunction generating mechanism and vibration diagnosis method on multi-plate clutch, " *Journal of Mechanical Engineering*, vol. 51, no. 1, pp. 117-122, 2015.

**Yuqing Feng** received the B.S. degree in Chongqing University of Technology, China, in 2018. He is currently working towards Ph.D. degree at School of Mechanical Engineering, Beijing Institute of Technology. His research focuses on fault diagnosis and health management of wet multi-disc clutches.

**Changsong Zheng** mainly presides over the development of transmission devices for multiple equipment projects, serving as the chief designer of transmission systems. His research directions include vehicle transmission reliability theory, hydraulic lubrication system pollution control, fault diagnosis, and intelligent operation and maintenance technology.

**Liang Yu** received the B.S. and Ph.D. degrees in mechanical engineering from Beijing Institute of Technology, Beijing, China. His research focuses on the theory and technology of special vehicles, as well as the theory of intelligent operation and maintenance of equipment and lifecycle performance prediction.

**Chengsi Wei** is mainly engaged in the overall design of armored vehicles and the research and development of transmission systems, including body structure design, transmission system fault diagnosis, the formulation of condition-based maintenance strategies, etc.

**Xiangjun Ouyang** is mainly engaged in the theoretical design and research and development of comprehensive transmission devices for special vehicles, and is engaged in the fields of intelligent operation and maintenance technology, fault diagnosis, fault prediction, and vehicle transmission reliability.